



NRL/FR/5620--94-9750

Infrared Hyperspectral Field Measurements of Seasonal Change at Wright-Patterson Air Force Base

WILLIAM A. SHAFFER
MARC R. SURETTE
MARTIN M. McHUGH

*Advanced Concepts Branch
Optical Sciences Division*

MICHAEL T. EISMANN
J. ROBERT MAXWELL
KENNETH K. ELLIS

*Environmental Research Institute of Michigan
Ann Arbor, Michigan*



19950217 034

December 30, 1994

REPORT DOCUMENTATION PAGE			Form Approved OMB No. 0704-0188	
Public reporting burden for this collection of information is estimated to average 1 hour per response, including the time for reviewing instructions, searching existing data sources, gathering and maintaining the data needed, and completing and reviewing the collection of information. Send comments regarding this burden estimate or any other aspect of this collection of information, including suggestions for reducing this burden, to Washington Headquarters Services, Directorate for Information Operations and Reports, 1215 Jefferson Davis Highway, Suite 1204, Arlington, VA 22202-4302, and to the Office of Management and Budget, Paperwork Reduction Project (0704-0188), Washington, DC 20503.				
1. AGENCY USE ONLY (Leave Blank)	2. REPORT DATE December 30, 1994	3. REPORT TYPE AND DATES COVERED		
4. TITLE AND SUBTITLE Infrared Hyperspectral Field Measurements of Seasonal Change at Wright-Patterson Air Force Base		5. FUNDING NUMBERS PE - 62111N PN - RU11G52		
6. AUTHOR(S) William A. Shaffer, Marc R. Surette, Martin M. McHugh, Michael T. Eismann,* J. Robert Maxwell,* and Kenneth K. Ellis*				
7. PERFORMING ORGANIZATION NAME(S) AND ADDRESS(ES) Naval Research Laboratory Washington, DC 20375-5320		8. PERFORMING ORGANIZATION REPORT NUMBER NRL/FR/5620-94-9750		
9. SPONSORING/MONITORING AGENCY NAME(S) AND ADDRESS(ES) Office of Naval Research Arlington, VA 22217-5660		10. SPONSORING/MONITORING AGENCY REPORT NUMBER		
11. SUPPLEMENTARY NOTES *Environmental Research Institute of Michigan, Ann Arbor, Michigan				
12a. DISTRIBUTION/AVAILABILITY STATEMENT Approved for public release; distribution unlimited.		12b. DISTRIBUTION CODE		
13. ABSTRACT (Maximum 200 words) Infrared spectra were collected of targets and tree and grass backgrounds during 9 days over a 2-month period, from September 24 to November 29, 1993, at Wright Laboratory/Wright-Patterson Air Force Base, Dayton Ohio. A description of the infrared spectrometer, the experiments conducted, and the data obtained are given. High spectral correlations in backgrounds were observed during the 2-month period, with the highest correlation observed near mid-day at the beginning of the 2-month period. There is evidence of seasonal variations in correlation as well as observed radiance. DTIC QUALITY INSPECTED 4				
14. SUBJECT TERMS Infrared Fourier transform spectrometer Field measurements Seasonal change		15. NUMBER OF PAGES 36		
		16. PRICE CODE		
17. SECURITY CLASSIFICATION OF REPORT UNCLASSIFIED	18. SECURITY CLASSIFICATION OF THIS PAGE UNCLASSIFIED	19. SECURITY CLASSIFICATION OF ABSTRACT UNCLASSIFIED	20. LIMITATION OF ABSTRACT SAR	

CONTENTS

1.	INTRODUCTION	1
2.	DATA COLLECTION INSTRUMENT	1
	Infrared Spectrometer	2
	Radiometric Calibration Equipment	3
	Azimuth/Elevation Mount	3
	Control and Data Acquisition System	4
	Boresight Video Equipment	4
3.	COLLECTION SITE, TARGET, AND EXPERIMENT DESCRIPTION	4
4.	DATA DESCRIPTION	10
5.	CONCLUSIONS	34
	REFERENCES	34

Accession For	
NTIS GRA&I	<input checked="" type="checkbox"/>
DTIC TAB	<input type="checkbox"/>
Unannounced	<input type="checkbox"/>
Justification	
By	
Distribution	
Availability Codes	
Dist	Avail and/or Special
A-1	

DISCLAIMER NOTICE



THIS DOCUMENT IS BEST QUALITY AVAILABLE. THE COPY FURNISHED TO DTIC CONTAINED A SIGNIFICANT NUMBER OF COLOR PAGES WHICH DO NOT REPRODUCE LEGIBLY ON BLACK AND WHITE MICROFICHE.

INFRARED HYPERSPECTRAL FIELD MEASUREMENTS OF SEASONAL CHANGE AT WRIGHT-PATTERSON AIR FORCE BASE

1. INTRODUCTION

Current military strategy has shifted away from a global engagement against a super-power enemy (the Soviet Union) to limited regional engagements against undetermined enemies. Consequently the task of military surveillance has shifted from the detection of ICBMs and bomber aircraft to critical mobile targets. Multispectral sensors offer the possibility of exploiting the spectral differences between targets and backgrounds as a detection discriminant. The Naval Research Laboratory (NRL) is a participant in a multiservice research program called the Joint Multispectral Program (JMSP) involving the Navy, Air Force, Army, and the Advanced Research Project Agency (ARPA). As part of this program, the JMSP has organized a number of field tests to obtain hyperspectral measurements of targets of interest in natural backgrounds. This paper describes an NRL-sponsored field-measurement effort, which took place at Wright Laboratory/Wright-Patterson Air Force Base during the fall of 1993.

Previous JMSP field measurements [1-2] of forest and grass backgrounds in summer (from the Redstone Arsenal tower operated by the U.S. Army Missile Command (MICOM)) have revealed high band-to-band spectral correlations. This observation implies that target detection with a spectral matched filter may be possible even if the single band contrast of the target to mean background is small. The MICOM data provide an existence proof for the infrared multispectral target detection problem.

A data collection effort was designed to investigate the diurnal and seasonal variations in background characteristics and the relationship of these variations to target detection. A series of measurements was made from the Building 620 tower at Wright Laboratory. Infrared hyperspectral signatures of targets and backgrounds were measured by using an infrared Fourier transform spectrometer (FTS) system. Data were collected under day and night conditions over a 9-week period at roughly 1-week intervals. The targets measured were military (M35 truck and a flat panel painted with a standard Army green coating) and reference (flat panels painted with coatings with useful spectral characteristics). Section 2 gives a description of the FTS. Section 3 details the data collection site and the experiments performed. Section 4 gives examples of the data and a preliminary discussion of the implications of the data.

2. DATA COLLECTION INSTRUMENT

The specifications for the data collection FTS were generated by the Environmental Research Institute of Michigan (ERIM) under the ARPA Multispectral Sensor Program (MSSP). The MSSP Program was tasked to investigate the utility of multispectral infrared techniques (sensors and data processing) for automated target detection. One of the results of the MSSP was a list of requirements

for an instrument capable of making fixed-site multispectral IR measurements with the required sensitivity to preserve the inherent spectral correlations of the natural backgrounds. These requirements were used by ERIM to develop a FTS system for ARPA.

The FTS system is composed of five primary components: the infrared spectrometer, radiometric calibration equipment, azimuth/elevation mount, control and data acquisition equipment, and boresight video equipment. Figure 1 is a block diagram of the entire system. The operation of the system is completely computer controlled so that the FTS can collect a large sequence of spectrally, spatially, and to some extent, temporally resolved radiance data of a scene in a time period limited almost completely by spectrometer sensitivity (integration time) requirements. The calibration and boresight video equipment are integrated into the system operation to provide radiometric calibration of the collected data and a visual record of each patch of target/background measured.

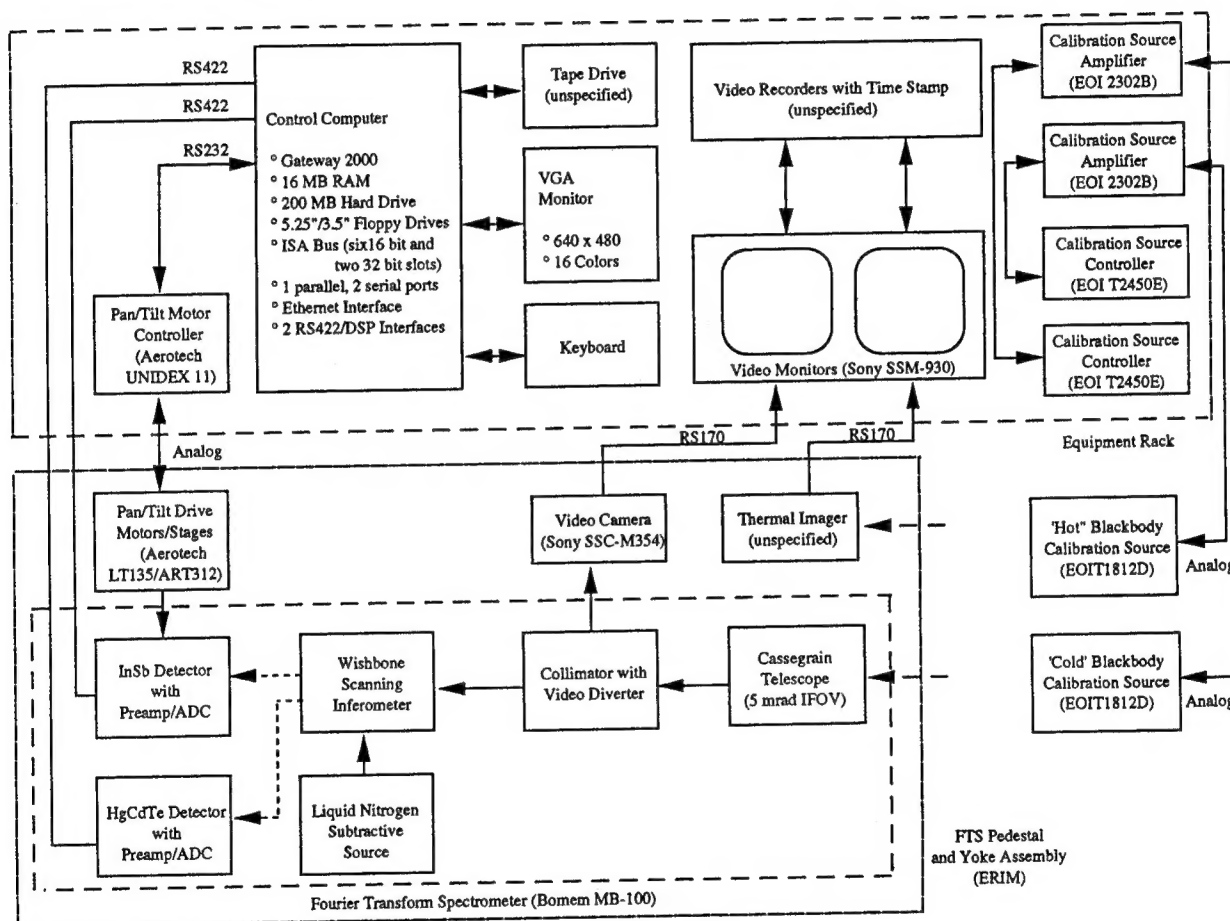


Fig. 1 — Field spectrometer system

Infrared Spectrometer

The spectrometer configuration selected for the field measurements is a Bomem MB-100 Fourier transform spectrometer. The basic interferometer design of the MB-100 consists of a KBr beamsplitter with two corner cube retroreflectors mounted on a wishbone scan arm. As the arm pivots, an optical path difference is introduced between the arms of the interferometer, thereby scanning out an interferogram. The spectrum is produced by sampling with a reference NeHe laser and Fourier transforming this interferogram.

The optical design of the interferometer provides two complementary inputs and outputs. In the configuration used, one of the inputs is directed to the target of interest while the other is directed to a stable cold (liquid nitrogen) reference. The outputs are directed to two separate detectors: an InSb detector for the midwave infrared (MWIR (3-5 μm)) spectral region and a HgCdTe detector for the longwave infrared (LWIR (8-12 μm)) region. Both of these detectors are located at image planes of the pupil plane of the spectrometer through a common field aperture and secondary field apertures in each set of output optics. These apertures can be adjusted to tradeoff MWIR/LWIR spatial registration with radiometric sensitivity and stability.

The input optics of the FTS consist of a 10-in. Cassegrain telescope and a collimator assembly. All focusing optics are reflective. With the field-limiting apertures open to their maximum diameter, the individual field of view (IFOV) of the sensor is 5 mrad. A dichroic beamsplitter in the collimating assembly provides an optical output to the charge coupled device (CCD) camera, which provides boresight video through the common-field-limiting aperture.

The FTS operates in a free-run mode and provides digital interferogram data through two separate interfaces (one for each detector). The interferogram is sampled in conjunction with an internal NeHe laser reference beam that propagates through the interferometer. An RS422 interface for each channel is used to allow remote data acquisition with the control computer. In addition, a digital signal processor (DSP) board (one for each channel) allows real time Fourier transformation of the acquired interferograms into complex spectra.

Radiometric Calibration Equipment

The spectrometer is calibrated in the field through a two-point complex calibration procedure developed by Revercomb [3]. This is accomplished by alternatively making measurements of two extended-area blackbody reference sources at different, known temperatures prior to each data collection sequence. In addition, such measurements can be repeated directly prior to and after each collection sequence to provide temporal calibration of linear FTS drift.

The calibration sources exhibit a 12 in. \times 12 in. blackbody surface controlled by a large (10 \times 10) array of matched thermoelectric modules with closed loop compensation in reference to a platinum-resistance thermometer on the emitting surface. The calibration sources have an accuracy of 0.03 C.

Azimuth/Elevation Mount

In order to acquire the correlation and contrast data of interest, it is necessary that the spectrometer be mounted on a pedestal with provisions for rapidly steering (under computer control) the line-of-sight to a sequence of predetermined locations. The configuration for the azimuth/elevation mount is a yoke assembly consisting of two motorized rotary stages mounted on a large tripod. The rotary stages provide extremely precise positioning via high-quality angular contact bearings and a precision oil-filled worm drive. Each of the stages is driven by a pulse-width modulated dc servo motor equipped with a rotary encoder to provide closed-loop position feedback and velocity stabilization. Motor control occurs via a digital controller, which allows point-to-point pan/tilt through either front-panel programming, a proportional speed joystick, or an RS232 interface. The yoke assembly was designed with adequate rigidity for 1 arc min stability.

Control and Data Acquisition System

The control and data acquisition system is field portable and capable of interfacing with the FTS motor controllers and all possible data analysis platforms. A PC-based system was required for FTS compatibility. Due to the large amount of data collected (on the order of 2 MB per experiment), it is essential that the system provide a rapid data acquisition capability, sufficient RAM and hard disk storage capacity, and a tape backup capability. The basic system is a PC with a 80486DX processor and 16 MB RAM equipped with several ISA boards to provide the FTS, motor controller, and network interfaces.

Boresight Video Equipment

Boresight video is required to set up the spatial scan sequence for an FTS data collection experiment and, during daytime hours, monitor and record a visual rendering of the measured target and background patches. A dichroic video diverter is included in the FTS collimator that allows a video camera to monitor the scene through the FTS telescope and front aperture. The mechanical interface is a C-mount. The collimator assembly contains the imaging optics.

3. COLLECTION SITE, TARGET, AND EXPERIMENT DESCRIPTION

The data collections were made from Building 620 at Wright Laboratory. This building has a 13-story tower that overlooks a wooded area. The tower has three floors of lab space at the top. Figure 2 shows the tower and surrounding area. The laboratory used was located on the 11 floor, approximately 150-ft above ground level. Figure 3 shows the FTS pointing out of the lab window. Figure 4 shows the FTS during calibration.

The lab faces due west, with the view opening out onto Loop Road, a small grassy area divided by a gravel road and a stand of deciduous trees approximately 784 ft away. The gravel road leads to a clearing within the trees. Figure 5 shows the test sight. Area B of the Air Force base can be seen in the background. Figure 6 is a ground-level view of the test sight. The orange trailer on the left houses a meteorological station. The various sensors can be seen spread around it. In the center are four reference panels and a radar-scattering camouflage net. The panels are coated with (from left to right) flame-sprayed aluminum, Krylon Ultraflat Black, and CARC 383 Green. The panel on the right side of the net is polished aluminum that has been allowed to oxidize. A more detailed description of the panels and their reflectance properties may be found in Ref 4. The M-35 truck is partially obscured by a tree on the right side of the picture.

The meteorological station support was provided by E-OIR, Inc. The station measures total precipitation, air temperature, dew point, visible (0.3 - 3 μm) and IR (3 - 50 μm) down-welling flux, air pressure, wind speed and direction, visibility, and ground temperature. The air temperature, dew point, and visibility sensors were all approximately 6 ft off the ground. The pyrometers, anemometer, and wind vane were approximately 9 ft off the ground. Data were collected continuously and averaged every 5 mins. Air temperature, relative humidity, pressure, wind speed, and wind direction were also monitored with a weather station provided by NRL. The anemometer and weather vane proved to be less sensitive than those operated by E-OIR, which required wind speeds greater than 3 mph before responding. These were located at a lower height of approximately 3 ft. Data were sampled once per minute with this station, without averaging. Additional ground truth was provided by FLIR, bore-sighted video and 35-mm camera imagery, regional meteorological data from the Base control tower, and thermistor temperature data from the panels.

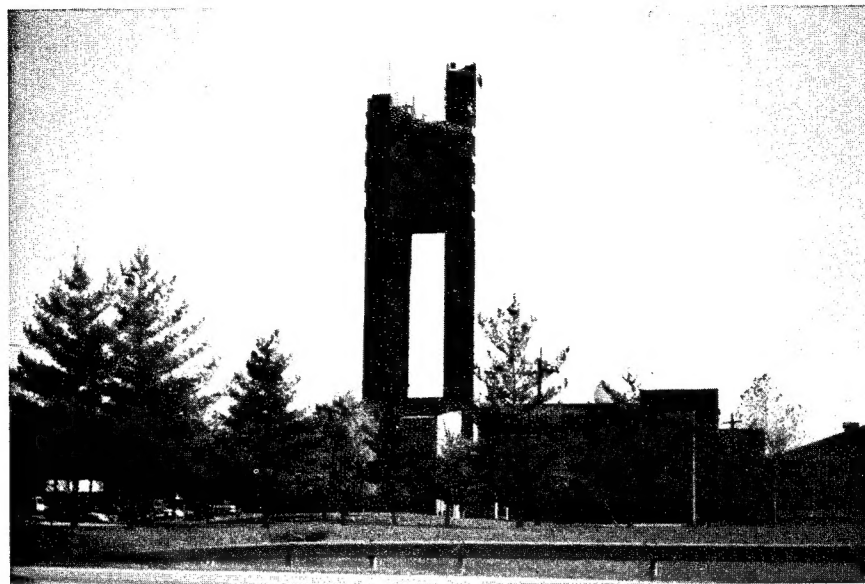


Fig. 2 — Building 620 tower at Wright-Patterson AFB, Dayton, Ohio

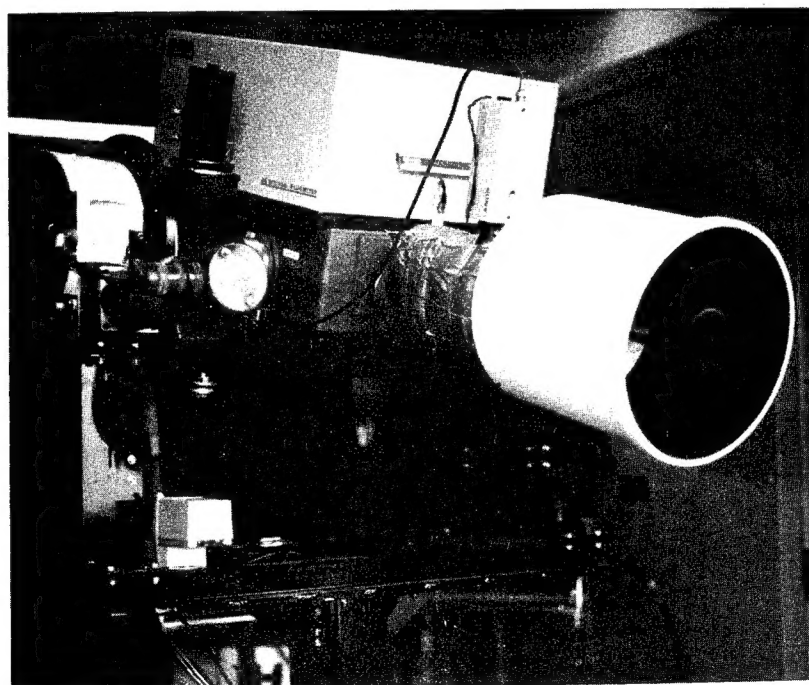


Fig. 3 — The spectrometer collecting data from the tower laboratory

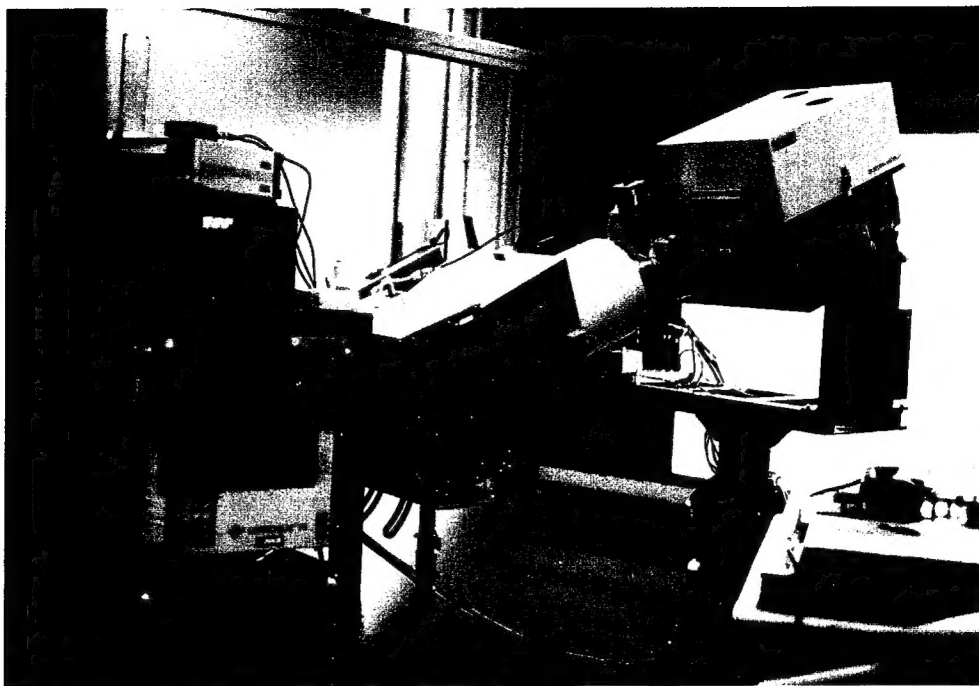


Fig. 4 — The spectrometer during the calibration procedure



Fig. 5 — The test site as seen from the tower laboratory, including test panels and the M-35 truck



Fig. 6 — The test site as seen from ground level

Figure 7 is a map of the test site drawn to scale showing the relative placement of the panels and meteorological station sensors. The truck was parked approximately 50 ft to the north of the specular panel. The panels were tilted approximately 15° from vertical, which is the nominal spectrometer depression angle. The azimuthal angles of the diffuse and painted panels were adjusted so that the panels were approximately perpendicular to the spectrometer's line-of-sight. These angles were measured to within $\pm 1^\circ$ relative to a line running north-south and are indicated on the map. The specular panel was pointed well away from the tower, the base of which is approximately 3° from due east so that it would reflect the sky back to the instrument and not an image of the tower. While the sun passed near the portion of the sky reflected to the spectrometer, the sun never actually came within the field of view (FOV).

The radar-scattering camouflage net was a diamond-shaped section of the Navy Stock Number 1080-00-103-1246 woodland camouflage screen kit. The point of the diamond was draped over a metal rod fastened to the tops of the specular and CARC panels. The front of the net was staked so that it hung nearly parallel to the panels. The remaining portion of the net was pulled back and stacked so that the instrument viewed a single layer of net. The net has two sides: spring-summer, which has various shades of green garnish, and fall-winter, which has various shades of green and brown garnish. The fall-winter side was deployed for all but one of the data collections.

Twelve different experiments were designed and repeated throughout the course of the collections. Each experiment had a different sample location or number of coadded scans. The different experiments are identified by a letter designation. Table 1 summarizes the experiment parameters. Subsets of the 12 experiments were combined into sequences. A typical day consisted of running a particular sequence repeatedly throughout the day, with each repetition given a sequence number. Each data set was given a unique name that contains the type of experiment, the date, and the sequence number during the day. For example, a patch on the left side of the tree canopy was designated as experiment "A." The data collected during the first sequence of the day on September 30 was labeled "A09301." The data collected at this same location during the second sequence were labeled "A09302," etc.

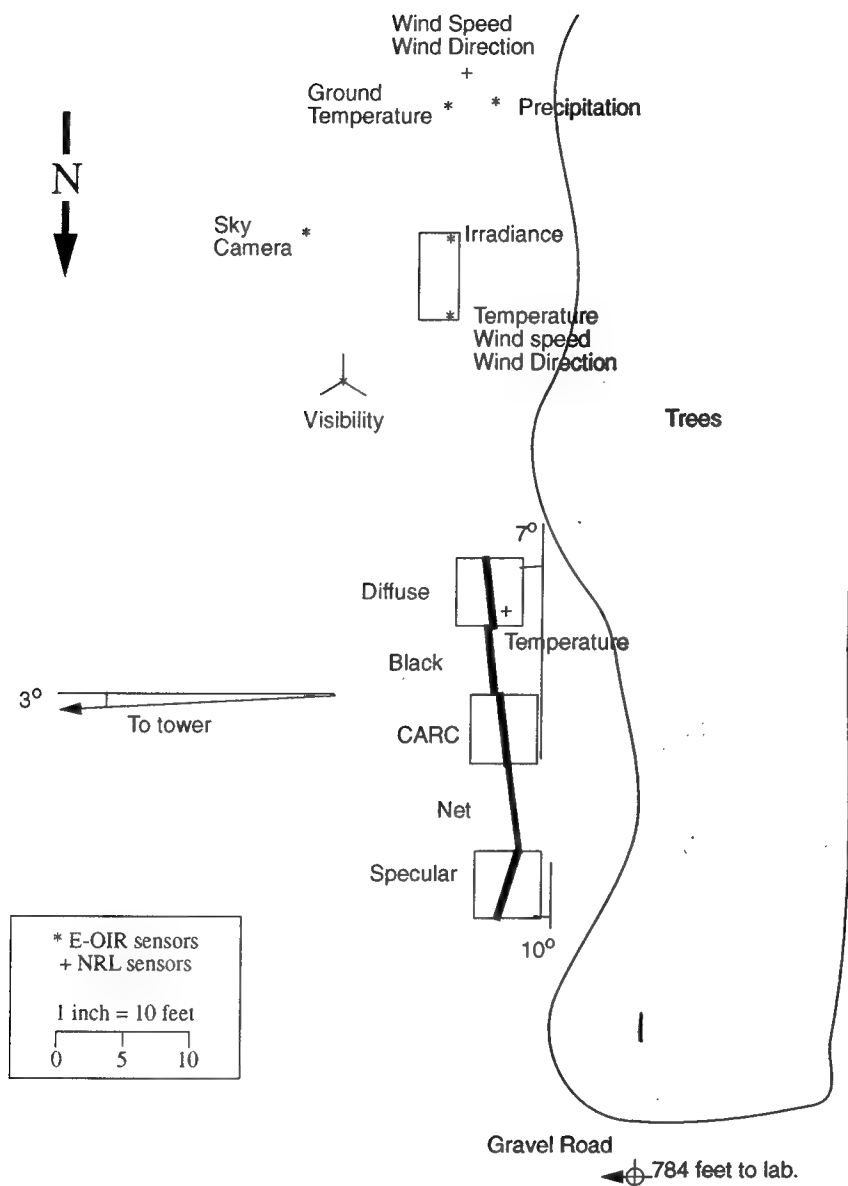


Fig. 7 — Test site

Table 1 — List of Experimental Parameters

Designation	Subject	Sample Geometry (V x H)	Sample Spacing (IFOVs)	# Co-adds	Purpose
A	tree canopy on left	6 x 6	2	25	spectral correlation
B	tree canopy on right	6 x 6	2	25	spectral correlation
C	grass	3 x 10	2	25	spectral correlation
D	trees in center	1 x 72	0.5	15	PSD correlation length
E	test panels/net	1 x 5	1.5	15	spectral contrast
	M-35 truck	9 pts.	1	15	
	trees	1 x 9	2	15	
	grass	1 x 9	2	15	
F	miscellaneous	-	-	15	spectral contrast
G	trees in center	1 x 72	0.5	5	PSD correlation length
H	test panels/net M-35 truck	1 x 5	1.5	15	spectral contrast
		9 pts.	-	15	
I	trees in center	1 x 72	1	5	PSD correlation length
J	asphalt road	-	-	15	spectral contrast
K	grass, leaves	-	-	15	spectral contrast
L	sky	5 x 1	8.7	15	sky radiance

Figure 8 shows the canopy and grass experiment locations and Figure 9 shows the locations on the truck that were measured. Figure 10 shows the net deployment.

Experiment F consisted of measurements of concrete and asphalt runways and several buildings, including the Air Force Museum hangers. Figure 11 is a photo of these targets, with the spectrometer FOV overlain.

A typical experiment consisted of five steps. First, the radiances of 20° C and 45° C blackbodies were measured. Second, another set of the blackbody radiances were measured and calibrated with the first set. Third, data were collected on targets and backgrounds of interest. These measurements typically took 20 to 30 measurements to collect. The instrument was found to drift significantly over time scales such as these [3]. Fourth, another set of blackbody radiances was collected and calibrated using the first set. Fifth, the second and third sets of blackbody radiances were used to perform a temporal calibration of the data that removes the linear component of the instrument drift. The data collected at each step were saved on disk.

4. DATA DESCRIPTION

In all, 243 experiments were performed. Table 2 summarizes the results. These measurements include observations of the same target and background over varying seasonal and environmental conditions. It is beyond the scope of this paper to give a thorough treatment of the data and the inferences that could be derived from analysis. However some examples are given that illustrate diurnal and seasonal variations in the observed data. A more complete analysis will be reserved for a future paper.

In general, the tree and grass backgrounds exhibit high band-to-band spectral correlations, although not as high as the correlations observed at MICOM [1]. Figure 12 is an example of the high spectral correlation. This sequence of measurements was taken of the B tree background on October 7. The measurements occurred between 8:40 a.m. and 8:30 p.m. For any individual experiment the observed spectral correlation between 9 and 11 μm is at least two 9's (i.e., $p > 0.99$). High spectral correlations are driven by large thermal contrasts. Therefore the highest correlation is observed at 11:26 a.m. when solar loading is a maximum. Because of the large temperature variation during the day, the effective correlation (the correlation computed assuming all of the data points were independent and measured simultaneously) of the entire sequence is four 9's. It is this high spectral correlation that allows the use of matched spectral filters to detect low contrast targets.

Figures 13 and 14 show two examples of low contrast targets. The first example (Fig. 13) is an observation of the CARC panel and tree canopy at 3:00 p.m. on October 22. At this time of day, the Sun has descended far enough so that most of the vegetation and the panels are in shadows. Without solar loading, the panels cool off faster than vegetation. The 3:00 p.m. data on October 22 caught the panel at the thermal crossover point (the point of near zero contrast between panel and background, which marks the transition from positive contrast in midafternoon and negative contrast at night). At thermal crossover, the observed radiance from the target at any one wavelength falls within the variation in observed background radiances. Consequently the mean single-color contrast between target and background is small. The contrast between the CARC panel and the tree canopy at either 8.5 or 10 μm is essentially zero (Fig. 13). Therefore a single color sensor using either 8.5 or 10 μm would fail to detect the CARC panel in the tree background. On the other hand, the spectral correlation between 8.5 and 10 μm for this background is high (0.997). Because of the high correlation in the background, it is possible to draw a decision boundary allowing the detection of the low contrast target.

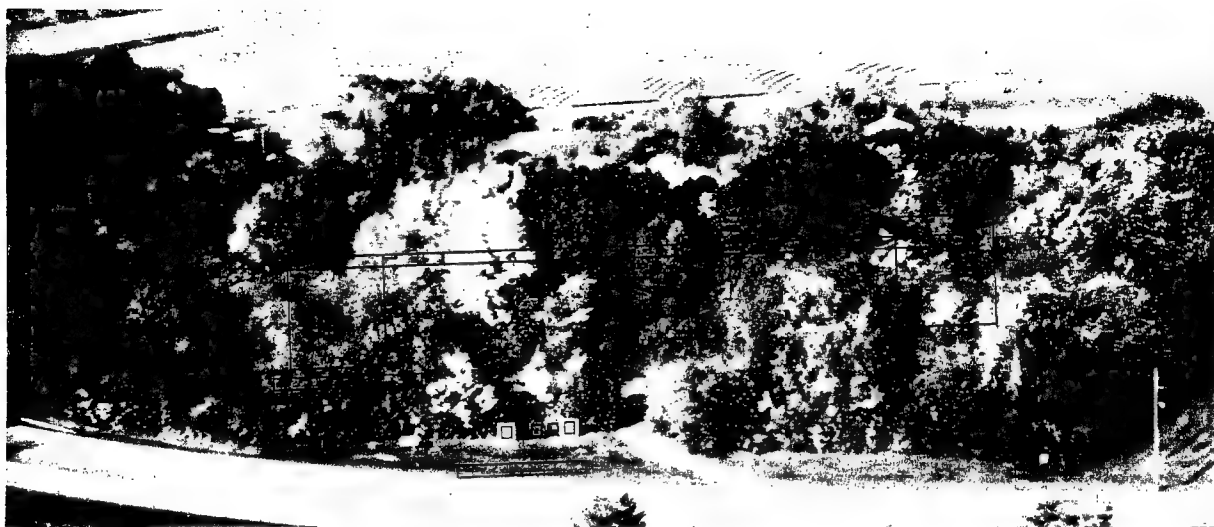


Fig. 8 — Experiment locations within the test site

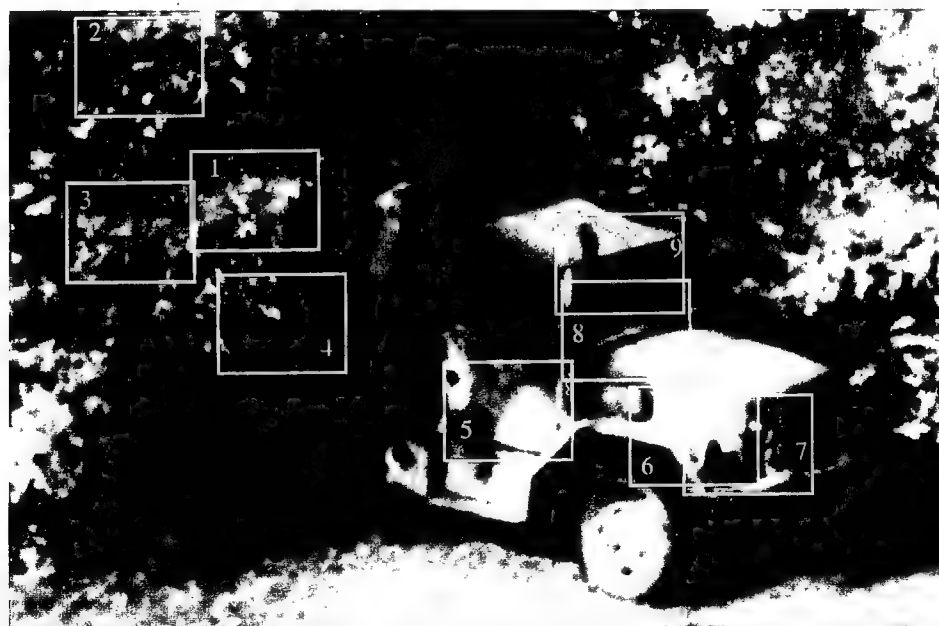


Fig. 9 — M-35 truck sample locations



Fig. 10 — Radar-scattering-net deployment



Fig. 11 — The nuclear reactor, hangers, and concrete runway behind the test site showing the approximate sample locations for Experiment F

Table 2 (Continues) — Summary of Wright Laboratory Collection Experiments

Date	Experiment	Type	Start Time	Target	Backgrounds	Ground Truth			Weather	Comments
						IR	Video	Met		
10-7-93	A10071	Correlation	5:35		trees	some		x	clear	
	D10071	PSD	6:00		trees	x		x	clear	IR only at end
	B10071	Correlation	6:20		trees	x		x	clear	
	E10071	Contrast	6:45	CARC, net, M35	trees, grass	x		x	clear	
	A10072	Correlation	7:00		trees	x		x	clear	
	B10072	Correlation	7:25		trees	x		x	clear	Sunrise
	E10072	Contrast	7:45	CARC, net, M35	trees, grass	x		x	clear	
	A10073	Correlation	8:00		trees	x		x	clear	Full sun
	D10073	PSD	8:20		trees	x		x	clear	
	B10073	Correlation	8:45		trees	x		x	clear	
	E10073	Contrast	9:20	CARC, net, M35	trees, grass	x		x	clear	
	A10074	Correlation	9:40		trees	x		x	clear	
	B10074	Correlation	10:00		trees	x		x	clear	Ken's hair in sample #17
	E10074	Contrast	10:20	CARC, net, M35	trees, grass	x		x	clear	Ken, Bill walked behind net during measurement
	A10075	Correlation	10:45		trees	x	x	x	clear	
	D10075	PSD	11:05		trees	x	x	x	clear	missed first 10 on video
	B10075	Correlation	11:30		trees	x	x	x	clear	
	E10075	Contrast	11:55	CARC, net, M35	trees, grass	x	x	x	clear	runners in grass meas'mnts
	C10075	Correlation	12:10		grass	x	x	x	clear	
	F10075	Spectral	12:50	Tgts of opp.			x		clear	not optimally focused
	A10076	Correlation	16:35		trees	x		x	clear	
	B10076	Correlation	16:55		trees	x		x	clear	
	E10076	Contrast	17:15	CARC, net, M35	trees, grass	x		x	clear	
	A10077	Correlation	17:35		trees	x	x	x	clear	
	D10077	PSD	18:00		trees	x	x	x	clear	sun low in sky directed toward sensor; blackbodies shielded during calibration and collection
	B10077	Correlation	18:25		trees	x	x	x	clear	
	E10077	Contrast	18:50	CARC, net, M35	trees, grass	x	x	x	clear	
	C10077	Correlation	19:10		grass	x	x	x	clear	
	A10078	Correlation	19:35		trees	x		x	clear	
	D10078	PSD	20:00		trees	x		x	clear	
	B10078	Correlation	20:20		trees	x		x	clear	
	E10078	Contrast	20:40	CARC, net, M35	trees, grass	x		x	clear	

Table 2 (Continues) — Summary of Wright Laboratory Collection Experiments

Date	Experiment	Type	Start Time	Target	Backgrounds	Ground Truth			Weather	Comments
						IR	Video	Panels		
10-22-93	A10221	correlation/contrast	5:47	CARC	trees	x		D,S,	clear	
	C10221	correlation	6:12		grass	x		T	clear	
	G10221	PSD	6:30		trees	x			clear	
	H10221	spectra	6:45	CARC		x		D,E,S,T	clear	
	I10221	PSD	6:51		trees	x			clear	
	B10222	correlation/contrast	7:07	CARC	trees	x		D,S,T	clear	
	E10222	contrast	7:30	CARC, net, M35	trees, grass	x		D,E,S	clear	sunrise
	G10222	PSD	7:40		trees	x			clear	
	H10222	spectra	7:55	CARC		x		D,E,S,T	clear	
	I10222	PSD	8:05		trees	x			clear	
	A10223	correlation/contrast	8:21	CARC	trees	x		D,S,T	clear	
	C10223	correlation	8:44		grass	x			clear	
	G10223	PSD	9:02		trees	x			clear	
	H10223	spectra	9:16	CARC		x		D,E,S,T	clear	
	I10223	PSD	9:23		trees	x			clear	
	B10224	correlation/contrast	9:39	CARC	trees	x		D,S,T	clear	
	E10224	contrast	10:02	CARC, net, M35	trees, grass	x		D,E,S,T	clear	
	G10224	PSD	10:16		trees	x			clear	
	H10224	spectra	10:31	CARC		x		D,E,S,T	clear	
	I10224	PSD	10:37		trees	x			clear	
	A10225	correlation/contrast	10:53	CARC	trees	x	x	D,S,T	clear	
	C10225	correlation	11:16		grass	x	x		clear	
	G10225	PSD	11:35		trees	x	x		clear	
	H10225	spectra	11:50	CARC		x	x	D,E,S,T	clear	
	I10225	PSD	11:58		trees	x	x		clear	
	B10226	correlation/contrast	12:14	CARC	trees	x	x	D,S,T	clear	
	E10226	contrast	12:39	CARC, net, M35	trees, grass	x	some	D,E,S,T	clear	video started late
	G10226	PSD	12:55		trees	x			clear	IR recorded throughout
	H10226	spectra	13:08	CARC		x	x	D,S,T	clear	
	I10226	PSD	13:15		trees	x			clear	

Table 2 (Continues) — Summary of Wright Laboratory Collection Experiments

Date	Experiment	Type	Start Time	Target	Backgrounds	Ground Truth				Weather	Comments
						IR	Video	Panels	Met		
10-22-93	A10227	correlation/contrast	14:08	CARC	trees	x		D,S,T	x	clear	panels in crossover
	C10227	correlation	14:39		grass	x			x	clear	
	G10227	PSD	14:52		trees	x			x	clear	
	H10227	spectra	15:16	CARC		x		D,E,S,T	x	clear	
	I10227	PSD	15:23		trees	x			x	clear	
	B10228	correlation/contrast	15:40	CARC	trees	x		D,S,T	x	clear	
	E10228	contrast	16:04	CARC, net, M35	trees, grass	x		D,E,S,T	x	clear	
	G10228	PSD	16:19		trees	x			x	clear	
	H10228	spectra	16:33	CARC		x		D,E,S,T	x	clear	
	I10228	PSD	16:40		trees	x			x	clear	
	A10229	correlation/contrast	16:56	CARC	trees	x		D,S,T	x	clear	
	E10229	contrast	17:20	CARC, net, M35	trees, grass	x		D,E,S,T	x	clear	truck in crossover
	G10229	PSD	17:38		trees	x		T	x	clear	sun low in sky directed
	H10229	spectra	17:52	CARC		x		D,E,S,T	x	clear	to sensor; blackbodies
	I10229	PSD	18:00		trees	x			x	clear	shielded during
	B1022A	correlation/contrast	18:16	CARC	trees	x		D,S,T	x	clear	collection
	C1022A	correlation	18:41		grass	x			x	clear	
	G1022A	PSD	19:01		trees	x			x	clear	
	H1022A	spectra	19:13	CARC		x		D,E,S	x	clear	sunset (at start)
	I1022A	PSD	19:20		trees	x			x	clear	
	A1022B	correlation/contrast	19:36	CARC	trees	x		D,S,T	x	clear	
	G1022B	PSD	19:58		trees	x			x	clear	
	H1022B	spectra	20:12	CARC		x		D,E,S,T	x	clear	
	I1022B	PSD	20:18		trees	x			x	clear	
	B1022C	correlation/contrast	20:33	CARC	trees	x		D,S	x	clear	
	E1022C	contrast	20:58	CARC, net, M35	trees, grass	x		D,E,S,T	x	clear	video started late
	G1022C	PSD	21:13		trees	x		T	x	clear	IR recorded throughout
	H1022C	spectra	21:26	CARC		x		D,S,T	x	clear	
	I1022C	PSD	21:33		trees	x			x	clear	

Table 2 (Continues) — Summary of Wright Laboratory Collection Experiments

Date	Experiment	Type	Start Time	Target	Backgrounds	Ground Truth				Weather	Comments
						IR	Video	Panels	Met		
11-9-93	A11091	correlation/contrast	5:18	CARC	trees	x		D,S,T	x	clear	
	C11091	correlation	5:42		grass	x			x	clear	
	H11091	PSD	5:59		trees	x			x	clear	
	G11091	spectra	6:12	CARC		x		D,E,S,T	x	mostly clear	
	I11091	PSD	6:18		trees	x			x	mostly clear	
	B11092	correlation/contrast	6:35	CARC	trees	x		D,S,T	x	mostly clear	
	E11092	contrast	7:04	CARC, net, M35	trees, grass	x		D,E,S,T	x	mostly clear	sunrise
	G11092	PSD	7:19		trees	x			x	mostly clear	
	H11092	spectra	7:31	CARC		x		D,E,S,T	x	mostly clear	
	I11092	PSD	7:37		trees	x			x	partly cloudy	
	A11093	correlation/contrast	7:52	CARC	trees	x	x	D,S,T	x	partly cloudy	
	C11093	correlation	8:15		grass	x	x		x	mostly cloudy	
	G11093	PSD	8:33		trees	x	x		x	mostly cloudy	
	H11093	spectra	8:46	CARC				D,E,S,T	x	mostly cloudy	
	I11093	PSD	8:51		trees	x	x		x	overcast	
	B11094	correlation/contrast	9:07	CARC	trees	x	x	D,S,T	x	overcast	
	E11094	contrast	9:30	CARC, net, M35	trees, grass	x	x	D,E,S,T	x	mostly cloudy	
	G11094	PSD	9:45		trees	x			x	mostly cloudy	
	H11094	spectra	9:58	CARC		x		D,E,S,T	x	mostly cloudy	
	I11094	PSD	10:03		trees	x			x	partly cloudy	
	A11095	correlation/contrast	10:19	CARC	trees	x		D,S,T	x	partly cloudy	
	C11095	correlation	10:42		grass	x			x	mostly clear	
	G11095	PSD	10:59		trees	x			x	clear	
	H11095	spectra	11:12	CARC		x		D,E,S,T	x	clear	
	I11095	PSD	11:18		trees	x			x	clear	
	H11096	spectra	11:33	CARC		x		D,E,S,T	x	clear	
	H11097	spectra	11:54	CARC		x		D,E,S,T	x	clear	panels vertical
	J11097	spectra	12:10	asphalt road		x			x	clear	no log file, not TC
	K11097	contrast	12:24		grass, leaves	x			x	clear	
	L11097	spectra	12:34		sky				x	clear	
	L11098	spectra	12:41		sky				x	clear	1 cm ⁻¹ resolution
	M11098	spectra	13:02		soil	x			x	clear	1 cm ⁻¹ resolution
	M11099	spectra	13:14	exhaust	soil	x			x	clear	1 cm ⁻¹ resolution

Table 2 (Continues) — Summary of Wright Laboratory Collection Experiments

Date	Experiment	Type	Start Time	Target	Backgrounds	Ground Truth				Weather	Comments
						IR	Video	Panels	Met		
11-22-93	E11221	contrast	6:00	CARC, M35	trees, grass	x		D,E,S,T	x	partly cloudy	
	H11221	spectra	6:15	CARC		x		D,E,S,T	x	partly cloudy	vertical panels D,E,S
	G11221	PSD	6:22		trees	x			x	partly cloudy	
	D11221	PSD	6:34		trees	x			x	partly cloudy	
	E11222	contrast	6:57	CARC, M35	trees, grass	x		D,E,S,T	x	partly cloudy	sunrise
	H11222	spectra	7:11	CARC		x		D,E,S,T	x	mostly clear	vertical panels D,E,S
	B11222	correlation/contrast	7:17	CARC	trees	x		D,S,T	x	mostly clear	
	C11222	correlation	7:40		grass	x		T	x	clear	
	E11223	contrast	7:57	CARC, M35	trees, grass	x		D,E,S,T	x	clear	vertical D,E,S panels in crossover
	H11223	spectra	8:11	CARC		x		D,E,S	x	clear	
	G11223	PSD	8:19		trees	x			x	clear	
	D11223	PSD	8:31		trees	x	x		x	clear	
	E11224	contrast	8:54	CARC, M35	trees, grass	x	x	D,E,S,T	x	clear	vertical panels, D,E,S*
	H11224	spectra	9:09	CARC			x	D,E,S,T	x	clear	missed pts 1-7 in video
	B11224	correlation/contrast	9:16	CARC	trees	x	x	D,S,T	x	clear	
	C11224	correlation	9:38		grass	x	x		x	clear	
	E11225	contrast	9:55	CARC, M35	trees, grass	x		D,E,S,T	x	clear	vertical panels, D,E,S
	H11225	spectra	10:10	CARC		x		D,E,S,T	x	clear	
	G11225	PSD	10:16		trees	x			x	clear	
	D11225	PSD	10:29		trees	x			x	clear	
	E11226	contrast	10:53	CARC, M35	trees, grass	x	x	D,E,S,T	x	clear	vertical panels, D,E,S
	H11226	spectra	11:08	CARC		x		D,E,S,T	x	clear	
	B11226	correlation/contrast	11:14	CARC	trees	x		D,S,T	x	mostly clear	
	C11226	correlation	11:36		grass	x			x	mostly clear	
	H11227	spectra	11:54	CARC		x		D,E,S,T	x	mostly clear	700-5000 cm ⁻¹
	L11227	spectra	12:06		sky				x	mostly clear	1 cm ⁻¹ resolution

* Truck locations shifted to left.

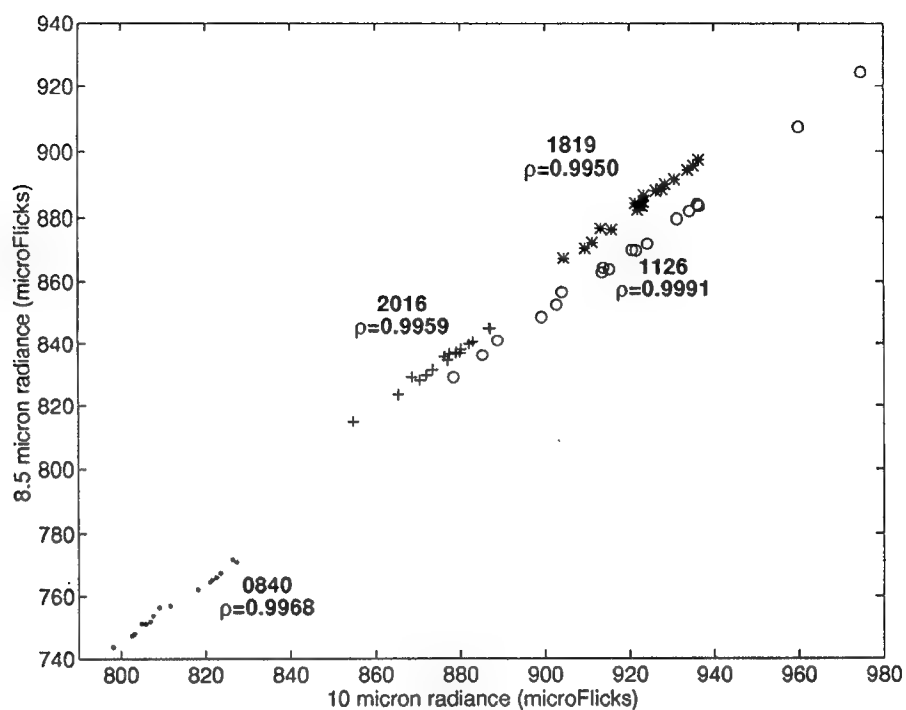


Fig. 12 — Scatter plot of the radiance at two wavelengths of a set of pixels containing tree canopy (Experiment B) at various times on October 7.

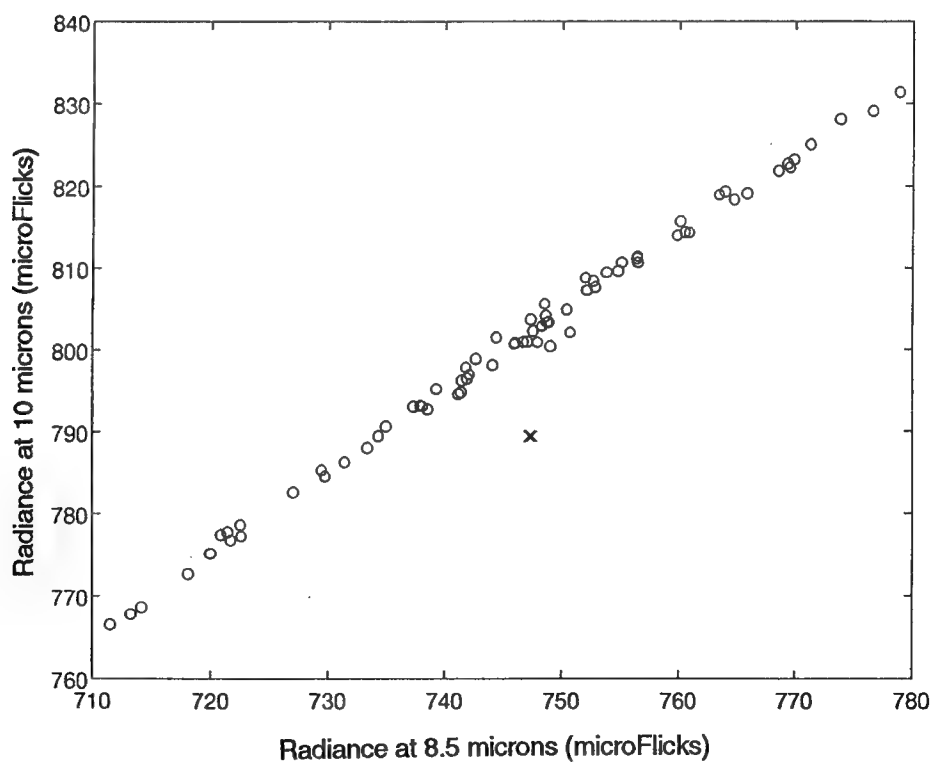


Fig. 13 — Low contrast example of the CARC panel in a tree background

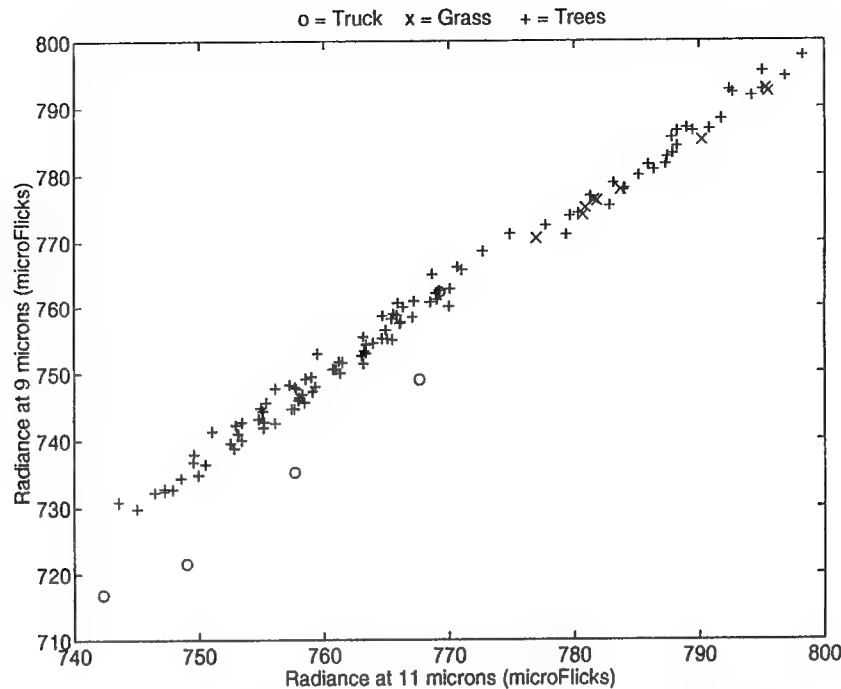


Fig. 14 — Low contrast example of the M-35 truck in a tree background

Figure 14 shows a second example. These measurements were of the M-35 truck and tree canopy at 4:00 p.m. October 22 (roughly the same time as the first example). The truck was an extended target allowing many pixels. There is some variability in the target pixel values due primarily to the differences in material in the pixels (painted metal, aluminum, glass, rubber, and canvas) and the geometric orientation of the truck parts. The contrast between three of the target pixels and the background are low. The two-color separation (using 9 and 11 μm) is large enough to allow detection. Notice that one target pixel lies within the background distribution even in two colors (the circle surrounded by pluses in Fig. 14). This pixel fell on the front windshield of the truck, which reflects the surrounding trees. Two-color detection based on this pixel alone would not be possible.

These two examples indicate that background spectral correlation can be an important property for target detection. This metric is important for many detection algorithms; for example, spectral-matched filtering. The stability of this parameter over time (diurnally as well as seasonally) is a key issue in the design of operational sensors that may rely on high spectral correlation for target detection. A primary motivation for measuring the same background pixels over time was to determine the variation of the spectral correlation. Spectral correlations were computed for six wavelength pairs for all of the A, B, and C experiments. The wavelength pairs (4.1 and 8.2 μm , 4.7 and 11 μm , 8.1 and 10.1 μm , 8.5 and 11 μm , 3.4 and 4.1 μm , 4.1 and 4.7 μm) were identified in the ARPA MSSP program [4] as candidate pairs for a dual-band sensor. Figures 15, 16, and 17 show plots of the correlations for the A, B, and C experiments, respectively. Correlations are usually highest near noon, with significant drop-off in the early morning and late afternoon. The spectral correlation is usually higher early in the year and lower later in the year. This may be caused as the leaves drop off the trees: the pixels then become composites of constituents at different ranges. The

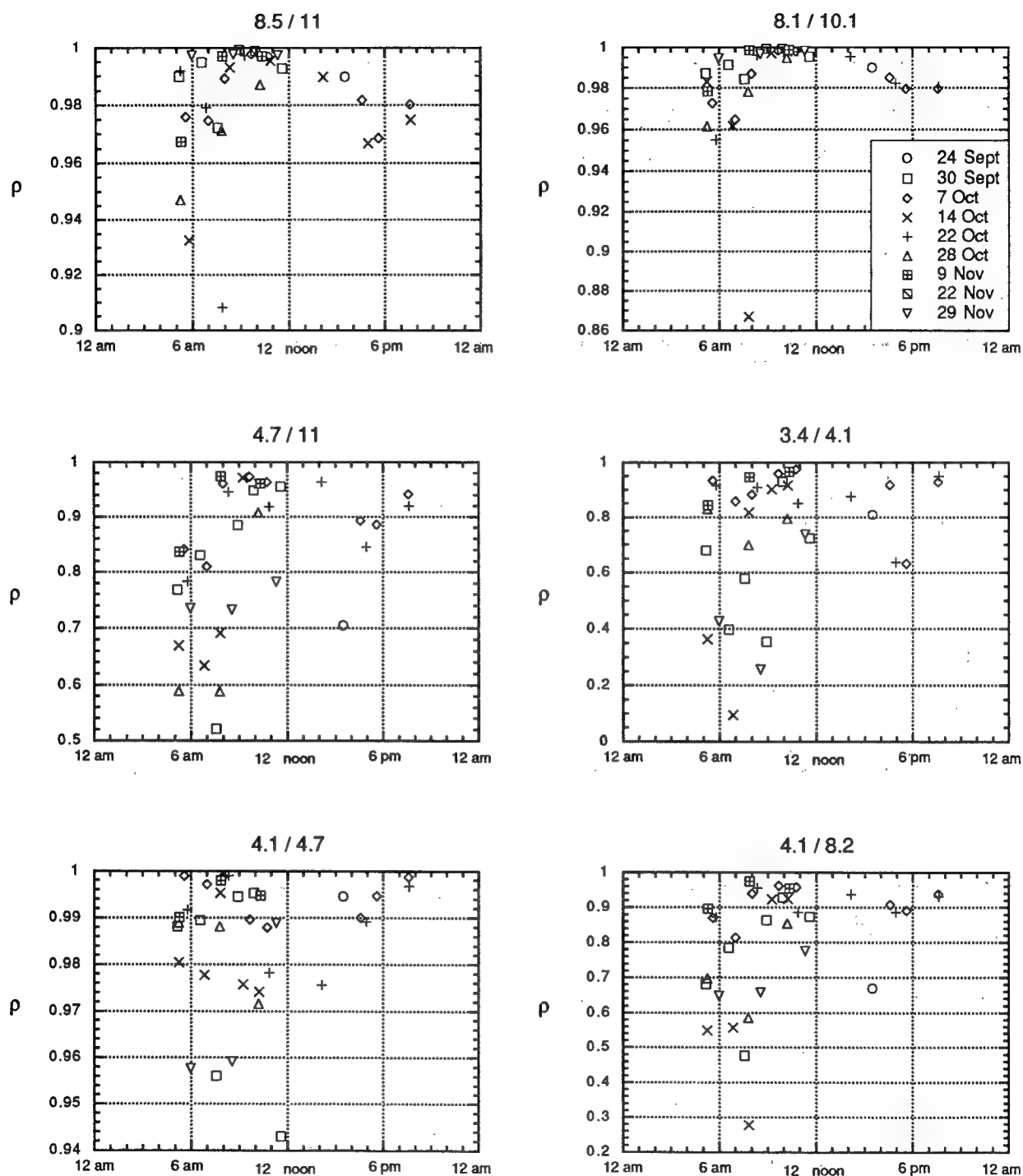


Fig. 15 — Diurnal and seasonal variation of spectral correlation in Experiment A for six waveband pairs

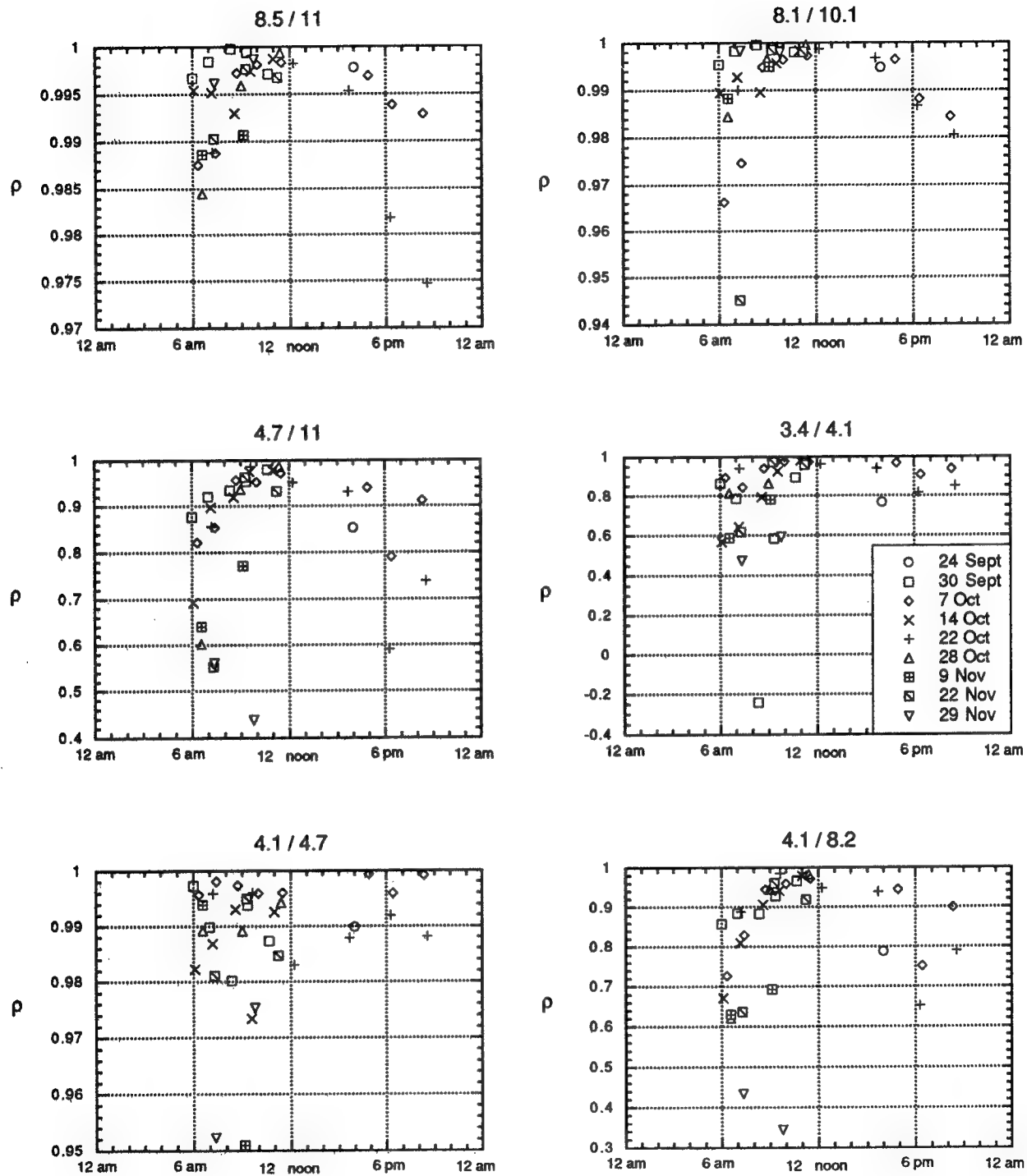


Fig. 16 — Diurnal and seasonal variation of spectral correlation in Experiment B for six waveband pairs

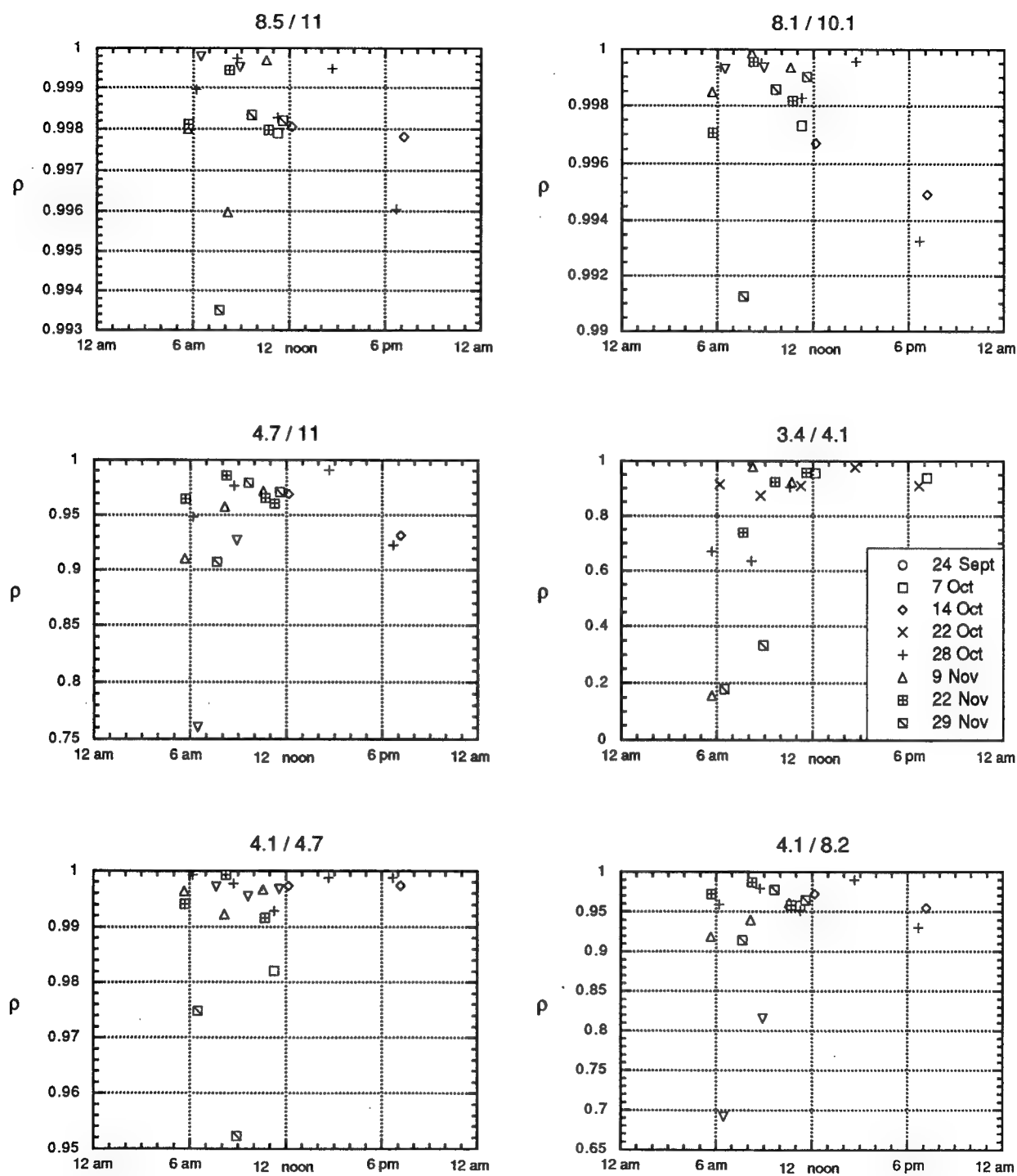


Fig. 17 — Diurnal and seasonal variation of spectral correlation in Experiment C for six waveband pairs

highest correlation is always observed for the grass (C) background. The best band pair (for correlation) was 8.5 and 11 μm . The correlations for this band pair for the three backgrounds as Fig. 18 shows. The correlations in A are consistently the worst and C the best. Background A was of a patch of trees that began to change color earlier than B. The exact relation between observed correlation and parameters (such as plant emissivity) is a subject for future investigation.

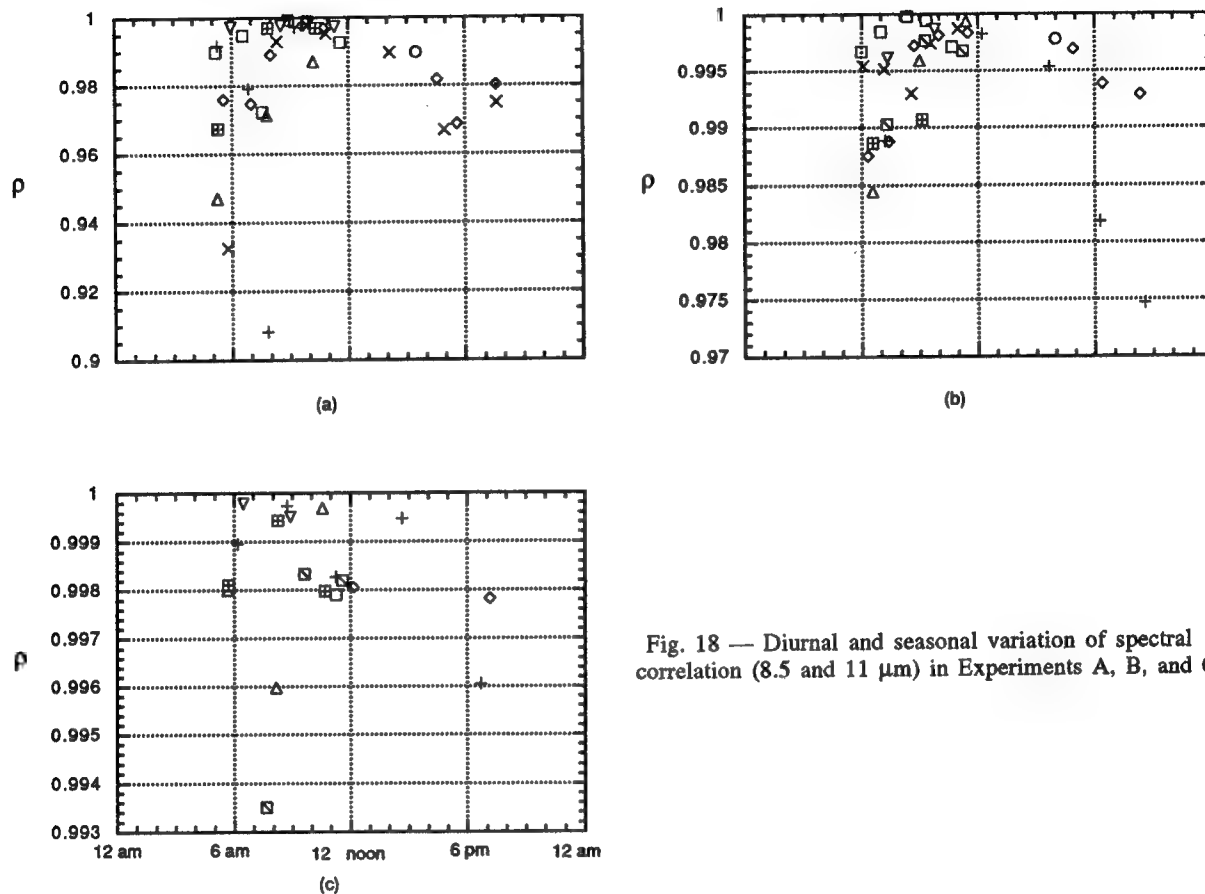


Fig. 18 — Diurnal and seasonal variation of spectral correlation (8.5 and 11 μm) in Experiments A, B, and C

Seasonal changes in the tree canopy were apparent in the photographs, IR imagery, and IR spectra. Figure 19 contains panoramic photos taken every week from September 24 to November 29. Note that areas covered by Experiments A and B change color and lose their leaves at different times. Figure 20 shows FLIR images taken at mid-morning on three days. The IR clutter increases as the leaves senesce and drop due to increasing variability in solar absorption and loss of the leaves' temperature-regulating capability. The ground in front of the tree has a very high radiance when compared to the canopy in the late fall. This is an area in which dead leaves are gathered. Apparently the high radiance is due to the fact that, without evaporating moisture or other biological regulation processes, the Sun heats the leaves to relatively high temperatures. The IR spectra also show seasonal variations. Figure 21 shows spatial plots of Experiment G at 8.5 μm on 6 days. These plots show large variations in spatial structure over time. The exact relationship between these variations and changes in emissivity or solar illumination has not yet been determined.

10/28/93



9370-4-2

11/9/93



9108-1-E

11/22/93



9108-1-9A

11/29/93



9369 3 6

Fig. 19 — Panoramic site photos from 30 September to 22 October 1993

9/30/93



93-11954-00

10/7/93



93-12319-8

10/14/93



93-12319-4

10/22/93



93-12319-1

Fig. 19 (Continued) — Panoramic site photos from 30 September to 22 October 1993

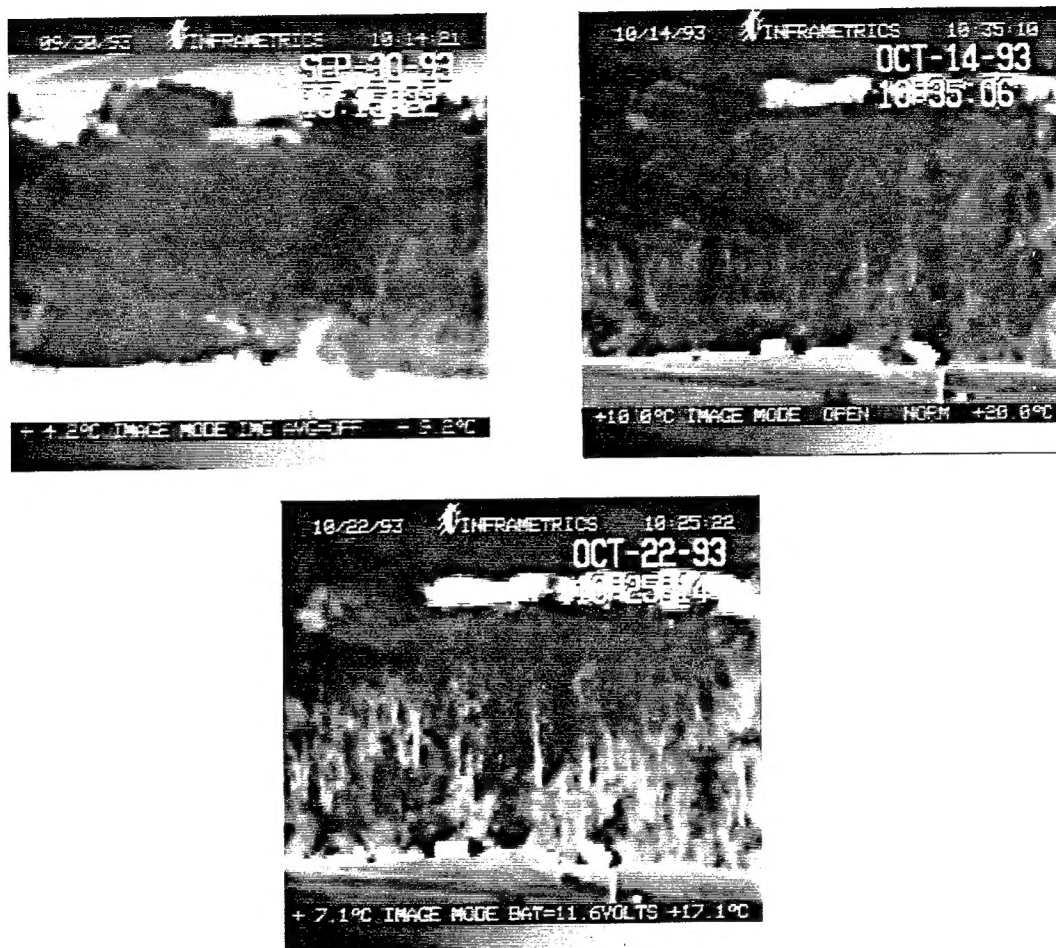


Fig. 20 — FLIR images of the test site showing the increasing clutter as the vegetation loses its leaves

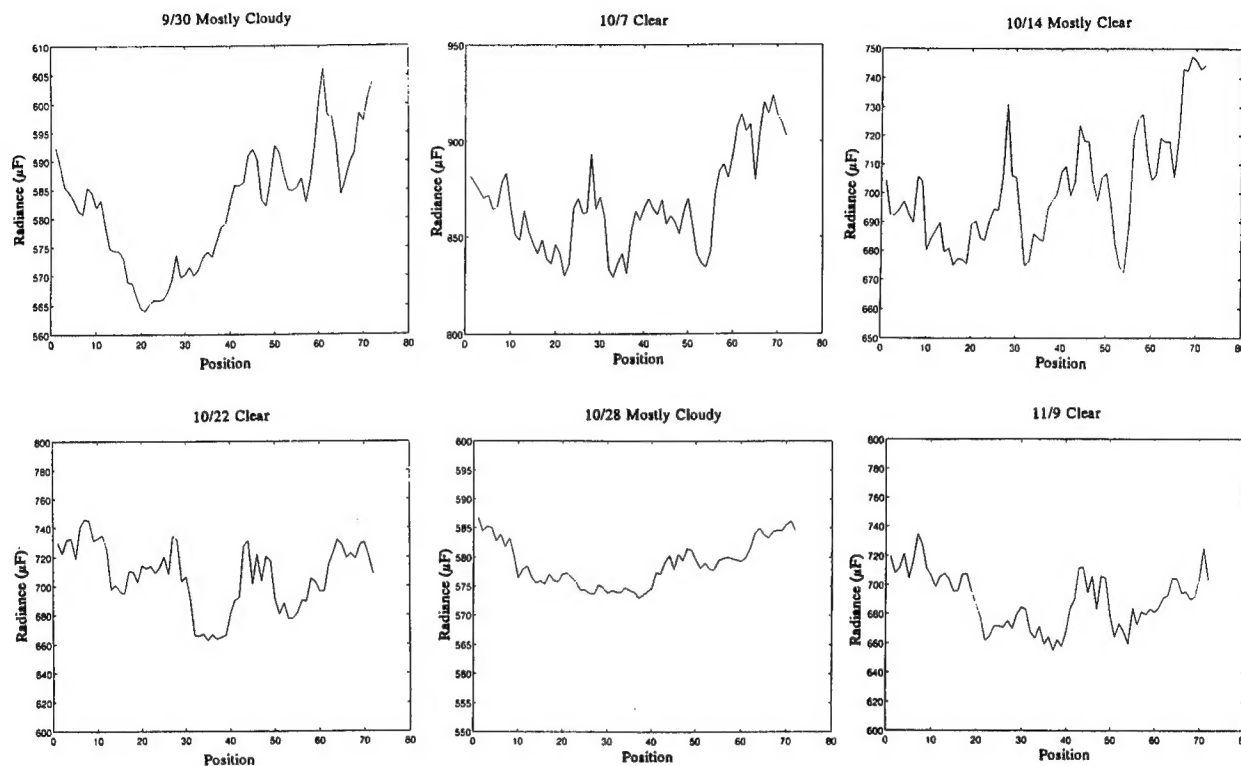


Fig. 21 — Seasonal variation in the spatial structure of the tree canopy (Experiment G)

5. CONCLUSIONS

IR spectra were collected of targets and tree and grass backgrounds during 9 days over a 2-month period. High spectral correlations in backgrounds were observed during this period with the highest correlation observed near mid-day, at the beginning of the 2-month period. There is evidence of seasonal variations in correlation and observed radiance. The phenomenological cause for such variations is the subject for future research on this data.

REFERENCES

1. M.T. Eismann, J. N. Cederquist, and C.R. Schwartz, "Infrared Multispectral Target/Background Field Measurements," Proceedings of the SPIE, **2235**, Orlando, FL, April 1994, pp. 130-147.
2. A.D. Stocker, A. Oshagan, J.H. Seldin, J.N. Cederquist, and C.R. Schwartz "Analysis of Multispectral Target/Background Field Measurements," Proceedings of the SPIE, **2235**, Orlando, FL, April 1994 pp. 148-161.
3. H.E. Revercomb, H. Buijs, H.B. Howell, D.D. LaPorte, W.L. Smith, and L.A. Sromovsky, "Radiometric Calibration of IR Fourier Transform Spectrometers: Solution to a Problem with the High-Resolution Interferometric Sounder," *Appl. Opt.* **27**, 3210 (1988).
4. J. Cederquist, M. Eismann, K. Ellis, J. Lange, T. Rogne, T. Schulz, C. Schwartz, J. Seldin, L. Basham, J. McNeil, D. Sofianos, W. Kendall, and A. Stocker, "Infrared Multipsectral Sensor Program, Phase I: Model-Based Performance Predictions," Final Report No. 232300-41-F , Environmental Research Institue of Michigan, 1993.